

# Diffusion Effect on the Anodic Reactions of Tungsten

Mustafa ANIK\*, Tuba CANSIZOĞLU and Sinem ÇEVİK  
Metallurgy Institute, Osmangazi University, 26480, Eskişehir-TURKEY  
e-mail: manik@ogu.edu.tr

Received 12.12.2003

Potentiodynamic and potentiostatic polarizations, and a rotating disk electrode technique were used to study the influence of diffusion on the anodic reactions of tungsten (W) in a broad pH range ( $\sim 0.3$ – $13.5$ ) in  $\text{H}_3\text{PO}_4$  buffered solutions. The anodic current was controlled totally by the kinetics of  $\text{H}^+$ -assisted dissolution below pH 1 (Region A). At around pH 2.5 (Region B), in addition to the kinetics of  $\text{H}_2\text{O}$ -assisted dissolution, specimen rotation had an effect on the current. This observation was attributed mainly to the physical damage to an oxide phase by hydrodynamic effects and partly to the diffusion of surface  $\text{H}_2\text{WO}_4(\text{aq})$  species. The anodic current was under the mixed control of the kinetics of  $\text{OH}^-$ -assisted dissolution and slow diffusion of surface  $\text{WO}_4^{2-}$  ions between pH 4 and 7 (Region C). The kinetics of the  $\text{H}_2\text{WO}_4(\text{s})$  solubilization and slow diffusion of surface  $\text{WO}_4^{2-}$  ions were observed to influence the anodic current between pH 7.5 and 11.5 (Region D). In highly alkaline solutions (pH  $> 12$ ; Region E), however, W anodic current was controlled totally by the slow diffusion of bulk  $\text{OH}^-$  ions to the electrode surface.

**Key Words:** Tungsten, Anodic Reactions, Diffusion

## Introduction

Tungsten (W) is a metal that shows very complex anodic behavior. In order to develop a unified theory for the anodic reaction of W, the oxidation and dissolution characteristics of W were investigated, and distinct pH regimes with the corresponding reaction mechanisms were identified in our previous studies<sup>1,2</sup>. Our research showed that surface oxides play a prominent role in the anodic reactions of  $\text{W}^{1,2}$  and some of these reactions are under partial or total diffusion control. Diffusion control on the W anodic reactions and its technological importance were also pointed out in several other publications<sup>3–5</sup>.

The current study extends our previous studies by focusing on the type of diffusing species in the W anodic reactions. For this purpose, potentiodynamic and potentiostatic polarization experiments with a rotating disk electrode are conducted over a wide pH range ( $\sim 0.3$ – $13.5$ ) in  $\text{H}_3\text{PO}_4$  buffered solutions at a constant ionic strength 1.4 M, and characteristics of diffusion in each pH regime are identified. The results gathered from this investigation are combined with our reported results to further our attempts to develop a unified theory for the anodic reaction of  $\text{W}^1$ .

---

\*Corresponding author

## Background

The total anodic oxidation reaction of W in acidic and weakly alkaline solutions can be expressed as in Equation 1<sup>9</sup>:



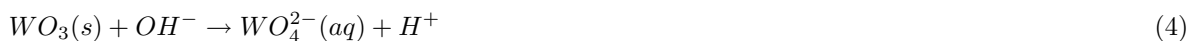
This oxidation reaction is followed by slow dissolution of the oxide phase<sup>1</sup>. Below pH 1 (Region A) dissolution is assisted by H<sup>+</sup> ions as in Equation 2<sup>1</sup>:



In the vicinity of pH 2.5 (Region B), which is identified as the point of zero charge (pzc) of the surface W oxide, dissolution is H<sub>2</sub>O-assisted as in Equation 3<sup>1</sup>:



Above the pzc (Region C), OH<sup>-</sup>-assisted dissolution is the main dissolution pathway (Equation 4<sup>1</sup>):



In the pH region 7.5 to 11.5 (Region D) pH-independent dissolution of the hydrated oxide phase takes place as in Equation 5<sup>1</sup>:



In strongly alkaline solution (pH > 12; Region E<sup>1</sup>), Kelsey<sup>10</sup> proposed the following reaction mechanism with Equation 7 being the rate-controlling reaction:



According to the reactions above, there are 5 distinct pH regimes (Regions A, B, C, D and E) and corresponding rate-controlling reactions (Reactions in Equations 2, 3, 4, 5 and 7) for W<sup>1</sup>.

## Experimental

### Materials

A W rod 0.4 cm in diameter (99.99% purity) was obtained from Aldrich. Reagent grade H<sub>3</sub>PO<sub>4</sub>, H<sub>2</sub>SO<sub>4</sub>, KOH and K<sub>2</sub>SO<sub>4</sub> were purchased from Aldrich. All the aqueous solutions were prepared from doubly distilled water. The water was deoxygenated by bubbling argon before experiments and purging was continued throughout the experiments. The test solutions were buffered using 0.1 M H<sub>3</sub>PO<sub>4</sub>, and pH was adjusted with H<sub>2</sub>SO<sub>4</sub> or KOH.

In order to calculate an ionic strength over a wide pH range, speciation diagrams for H<sub>3</sub>PO<sub>4</sub> and H<sub>2</sub>SO<sub>4</sub> were generated as shown in Figures 1 and 2, respectively. Activity coefficients of related ionic species were

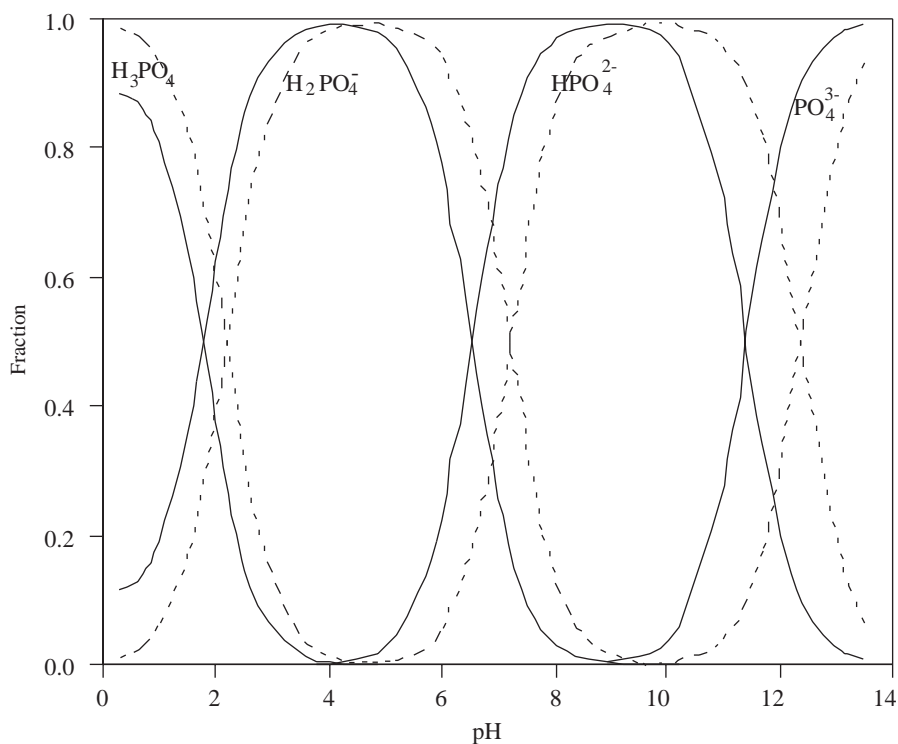


**Figure 1.** Speciation diagram for  $\text{H}_3\text{PO}_4$ . Solid lines take into account the activity coefficients tabulated in Table 1. Light dashed lines are for infinitely dilute solutions.

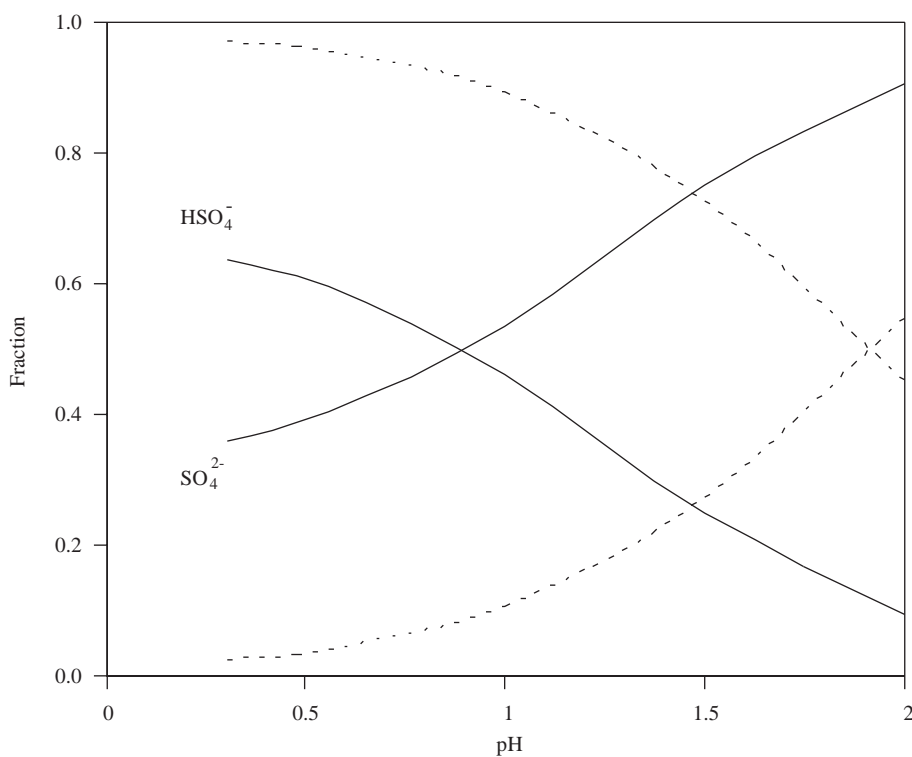


**Figure 2.** Speciation diagram for  $\text{H}_2\text{SO}_4$ . Solid lines take into account the activity coefficients tabulated in Table 1. Light dashed lines are for infinitely dilute solutions.

calculated according to the Pitzer model<sup>11</sup> by considering only the binary interactions (Table 1). Activity coefficients of neutral species and water were assumed to be 1. In the speciation diagrams (Figures 1 and 2) the light dashed lines show the corresponding speciation for the infinitely dilute solutions (for the case that all activity coefficients are 1). Ionic strength was fixed at 1.4 for all test solutions by adding the required amount of  $K_2SO_4$ . The composition of the test solutions used in this investigation and the corresponding measured pH values are given in Table 2.

**Table 1.** Activity coefficients of various ions. Pitzer model is used by considering only the binary interactions<sup>11</sup>.

$H_2PO_4^-$	$HPO_4^{2-}$	$PO_4^{3-}$	$HSO_4^-$	$SO_4^{2-}$
0.39	0.09	0.01	0.55	0.06

**Table 2.** Compositions of the test solutions with corresponding measured pH values. Concentrations are in molarity and ionic strength is fixed at 1.4 M.

Sol. no	$H_3PO_4$	$H_2SO_4$	KOH	$K_2SO_4$	pH
1	0.100	1.000	–	0.120	~ 0.3
2	0.100	0.800	–	0.180	~ 0.5
3	0.100	0.500	–	0.300	0.7
4	0.100	0.320	–	0.310	1.0
5	0.100	0.150	–	0.380	1.5
6	0.100	–	–	0.460	2.1
7	0.100	–	0.050	0.440	2.4
8	0.100	–	0.070	0.430	2.6
9	0.100	–	0.090	0.420	2.9
10	0.100	–	0.105	0.420	3.6
11	0.100	–	0.110	0.410	4.5
12	0.100	–	0.118	0.410	5.2
13	0.100	–	0.134	0.390	6.0
14	0.100	–	0.170	0.360	6.8
15	0.100	–	0.200	0.340	7.3
16	0.100	–	0.210	0.330	7.8
17	0.100	–	0.228	0.320	8.4
18	0.100	–	0.231	0.320	9.5
19	0.100	–	0.235	0.310	10.2
20	0.100	–	0.253	0.290	11.0
21	0.100	–	0.285	0.250	11.7
22	0.100	–	0.350	0.210	12.5
23	0.100	–	0.450	0.170	13.1
24	0.100	–	0.800	0.050	13.5

## Methods

The W electrode used in the electrochemical experiments was embedded in a cylindrical piece of Teflon. To block the crevice between the Teflon holder and the electrode, epoxy was applied and subsequently allowed to harden in a vacuum. The exposed electrode surface ( $0.126 \text{ cm}^2$ ) was ground with 1200 grit grinding paper and polished with  $1 \mu\text{m}$  diamond paste just prior to each experiment. The polished electrode was rinsed with acetone and doubly distilled water to eliminate traces of diamond paste from the surface. Following

this cleaning, the electrode was kept in 5 M KOH solution for 1 min and then rinsed again with doubly distilled water to dissolve air-formed oxide (as much as possible without getting a roughened surface) on the W. Special care was taken to keep the time as short as possible (< 1 min) between polishing the specimen and inserting it into the test cell.

A standard 3-electrode system consisting of a working electrode (W), a counter electrode (carbon rod; 0.6 cm in diameter), and a reference electrode (saturated calomel electrode) was used. A Gamry model PC4/300 mA potentiostat/galvanostat controlled by a computer with DC105 DC Corrosion Analysis software was used in the electrochemical measurements. Rotating disc electrode (RDE) experiments were carried out using an EG& G model 616 rotating assembly. The electrical connection was provided from the back of the electrode by attaching it to the RDE assembly. All experiments were performed in a 800 ml glass cell.

Potentiodynamic polarization curves were generated by sweeping the potential from open circuit potential (OCP) to 1.2 V at a scan rate of 1 mV s<sup>-1</sup> with 0 and 1000 rpm rotations. Each polarization experiment was run after holding the electrode for 1 h at the open circuit potential to allow steady-state to be achieved. Potentiostatic polarizations were carried out at both 300 mV (SCE) and 1 V (SCE) under rotation, which was varied between 0 and 2500 rpm (0, 300, 500, 1000, 1500, 2000 and 2500 rpm). After each rpm increment, the electrode was held at the working electrode long enough to obtain steady-anodic current.

Unless indicated otherwise, all potentials refer to the saturated calomel reference electrode, SCE (SCE, +0.241 V vs. SHE). All experiments were conducted at laboratory temperature (20 ± 1 °C).

## Results and Discussion

### Potentiodynamic Polarization Experiments

The anodic polarization behavior of W for stationary (0 rpm) and rotating (1000 rpm) specimens at various pH values is shown in Figure 3. The effects of pH on the current vs. potential trends in this figure have been reported previously<sup>1</sup>. In this study, however, the emphasis is on the effects of rpm on the anodic currents of W. Except at pH 0.5, at all pH values the anodic current increases with the specimen rotation in a pseudo plateau current region. Depending on the applied potential in this plateau region the specimen rotation has varying influence on the current in acidic and weak alkaline solutions (pH 2.6, 5.2 and 8.4). In strong alkaline solution (pH 13.5), however, there is a very well-defined anodic limiting current.

### Potentiostatic Polarization Experiments with a Rotating Disk Electrode

The effect of specimen rotation on the anodic reactions of W can be identified more clearly if the rotation dependence characteristics of the steady-state anodic currents are determined in each distinct pH regime. For this purpose the steady-state anodic currents are obtained at 300 mV and 1 V, which are the characteristic potentials of the pseudo plateau regions in Figure 3, for the specimen rotations of 0, 300, 500, 1000, 1500, 2000 and 2500 rpm, and some of them are shown in Figures 4a, 4b, 5a and 5b. Not all the steady-state currents gathered from this investigation are given in these figures to allow clear presentation. All data obtained at 300 mV and 1 V, however, are shown in Figures 6 and 7, respectively, for 0, 500 and 2000 rpm.

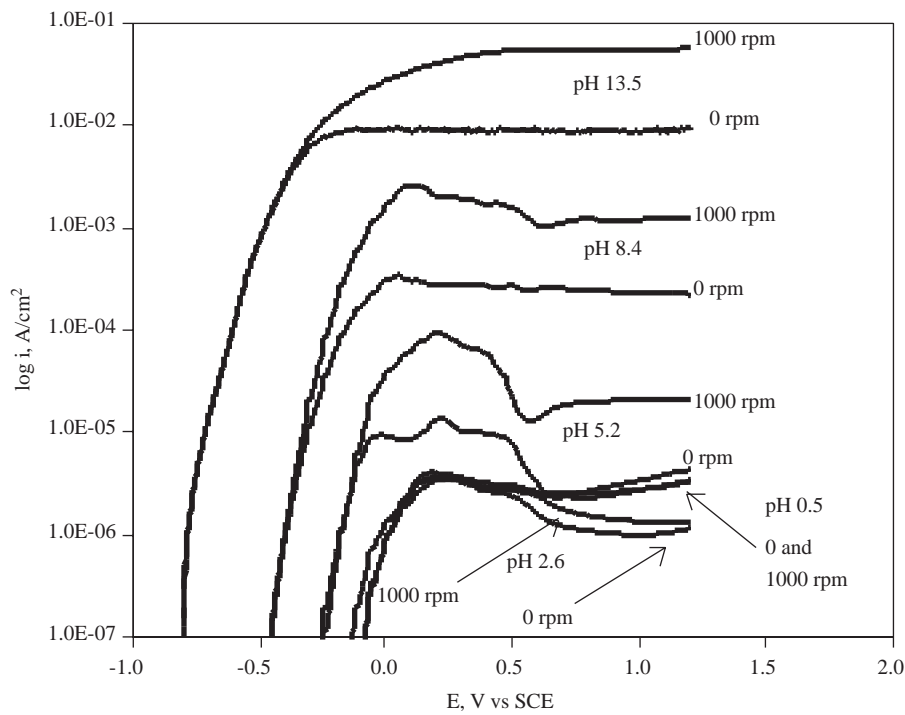


**Figure 3.** Effect of rpm on the potentiodynamic anodic polarization behavior of W at various pH values.

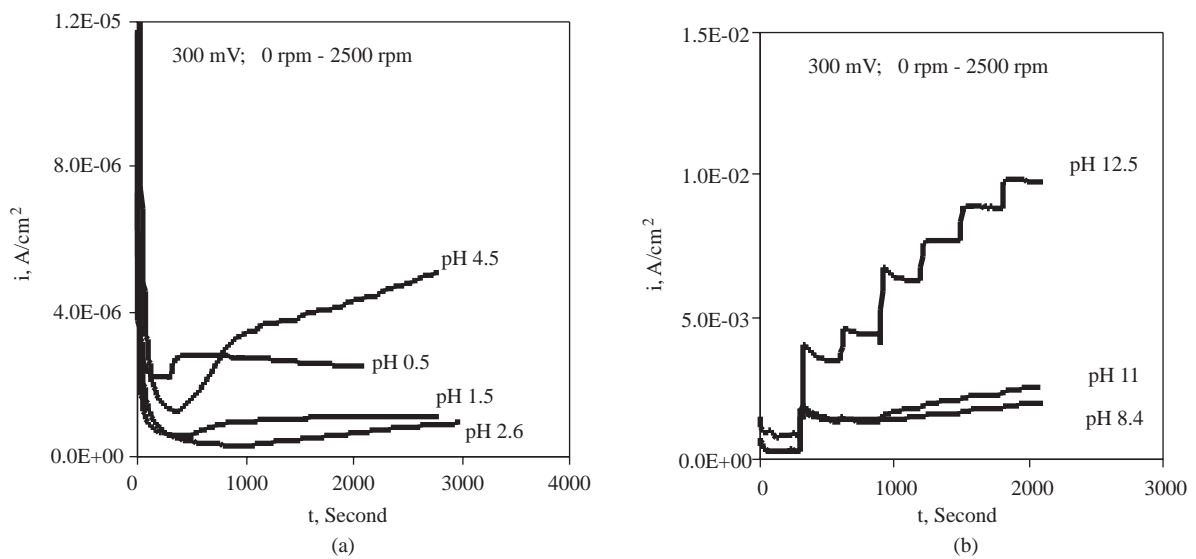


**Figure 4.** Effect of specimen rpm on the steady-state currents obtained at 300 mV for pH (a) 0.5, 1.5, 2.6 and 4.5, (b) 8.4, 11 and 12.5.

Except in Region A, in all regions specimen rotation has a significant influence on the steady-state current in Figures 6 and 7. The increase in current mainly takes place upon switching the electrode from stationary (0 rpm) to rotating (500 rpm). A further increase in rotation (500 rpm to 2000 rpm) causes a considerable increase in current only in Regions D and E.

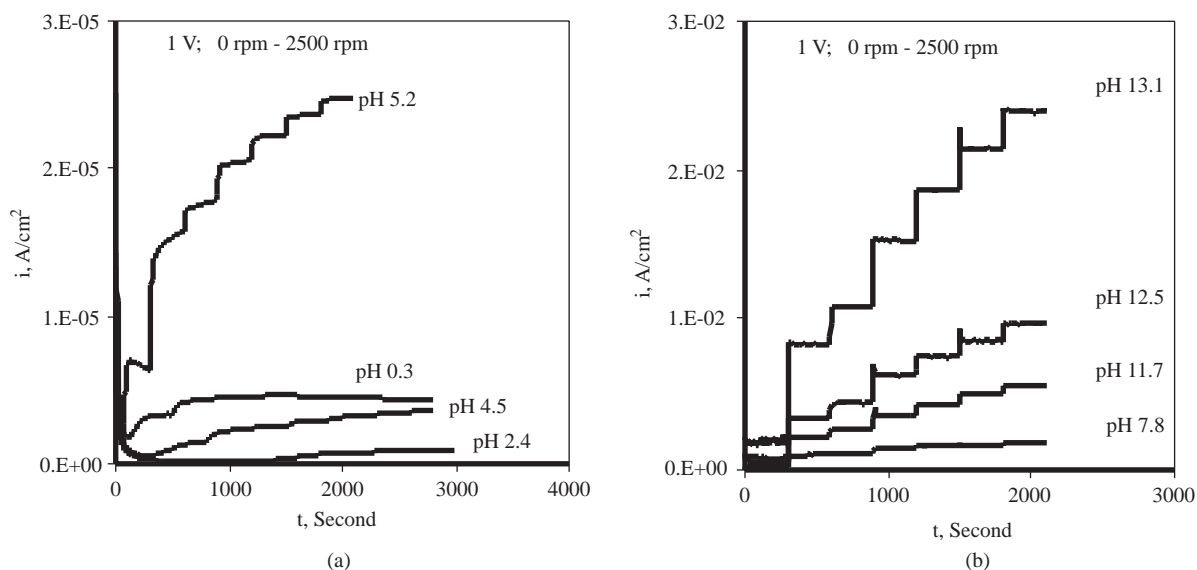


**Figure 5.** Effect of specimen rpm on the steady-state currents obtained at 1 V for pH (a) 0.3, 2.4, 4.5 and 5.2, (b) 7.8, 11.7, 12.5 and 13.1.

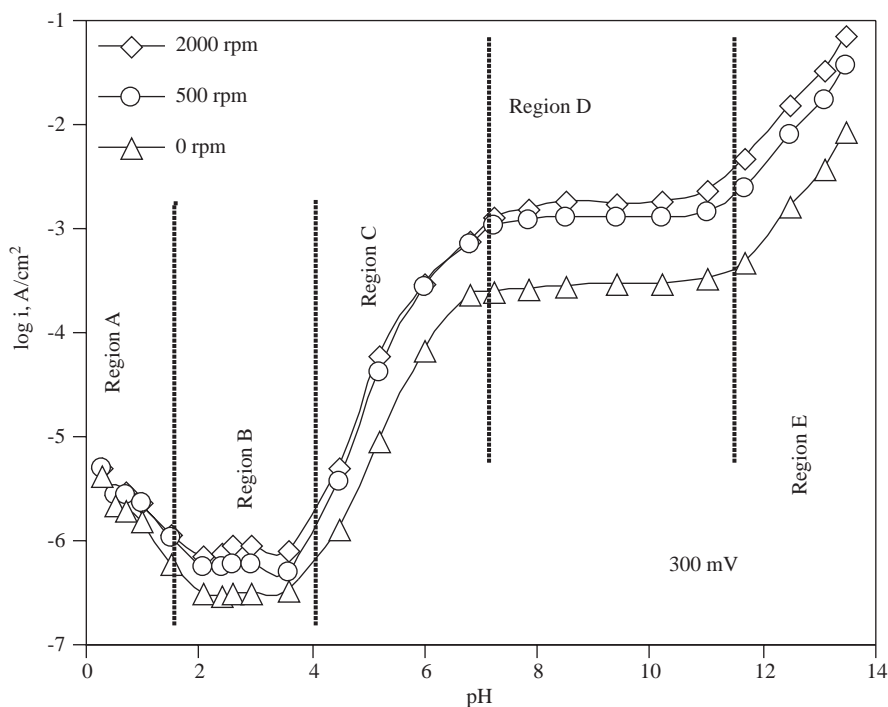


**Figure 6.** The rpm dependence of the steady-state currents at 300 mV in different pH regimes.

The dependence of the steady-state current on the specimen rotation for 1 V is shown in Figures 8a, 9a, 10a, 11a and 12a for Regions A, B, C, D and E, respectively. The relevant data in these figures are picked from current vs. time curves as some of them are given in Figures 5a and 5b. The corresponding Koutecky-Levich ( $i^{-1}$  vs.  $w^{-1/2}$ ) plots are given in Figures 8b, 9b, 10b, 11b and 12b. These plots are defined by Equation 8 for a first order reaction<sup>12,13</sup>:

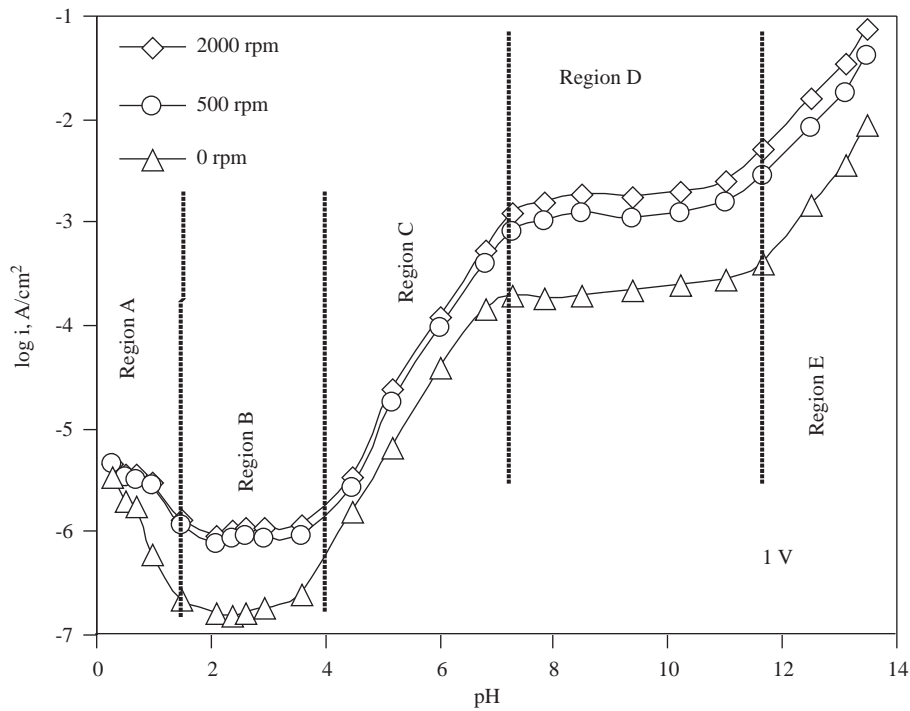


**Figure 7.** The rpm dependence of the steady-state currents at 1 V in different pH regimes.

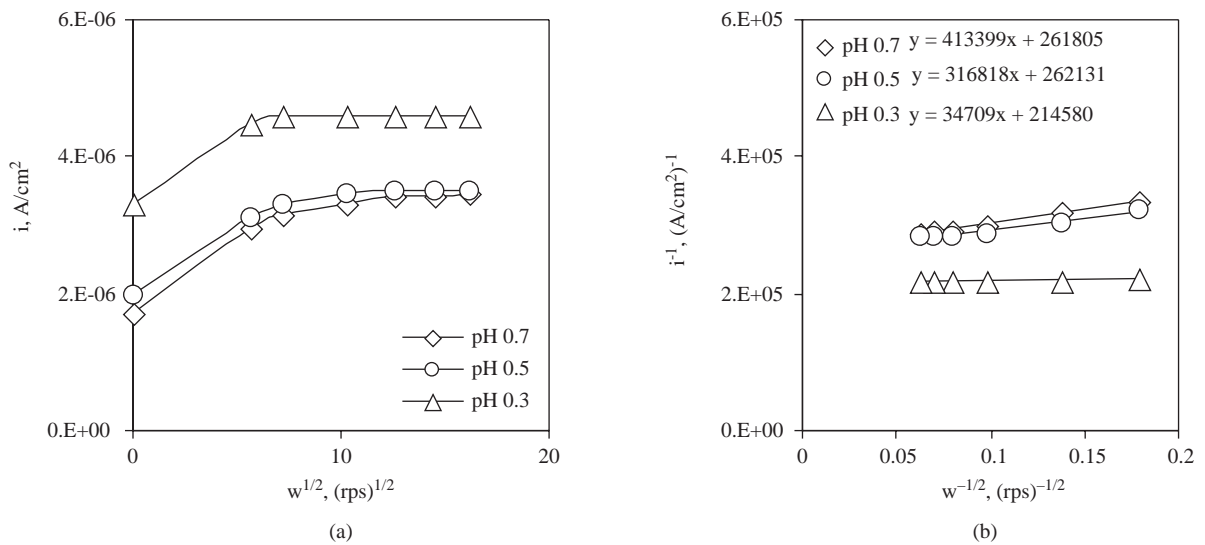


**Figure 8.** (a) Effect of specimen rotation on the steady-state currents in Region A. (b) Corresponding Koutecky-Levich plots.

$$\frac{1}{i} = \frac{1}{i_K} + \frac{1}{i_D} \quad (8)$$

where  $i_K$  and  $i_D$  represent the kinetic- and diffusion-limited parts of the anodic current density, respectively. Equations 9 and 10 provide expressions for  $i_K$  and  $i_D$ , respectively:

$$i_K = nFkC \quad (9)$$

$$i_D = 0.62nFD^{2/3}\nu^{-1/6}Cw^{1/2} \tag{10}$$

where  $n$  is the total number of electrons (eq. mol<sup>-1</sup>),  $F$  is the Faraday constant (96480 C eq.<sup>-1</sup>),  $k$  is the apparent rate constant (cm s<sup>-1</sup>),  $C$  is the concentration of the reactant (mol cm<sup>-3</sup>),  $D$  is the diffusion coefficient of the reactant (cm<sup>2</sup>s<sup>-1</sup>),  $\nu$  is the kinematic viscosity (0.01 cm<sup>2</sup>s<sup>-1</sup> for water<sup>13</sup>) and  $w$  is the angular velocity (s<sup>-1</sup>).

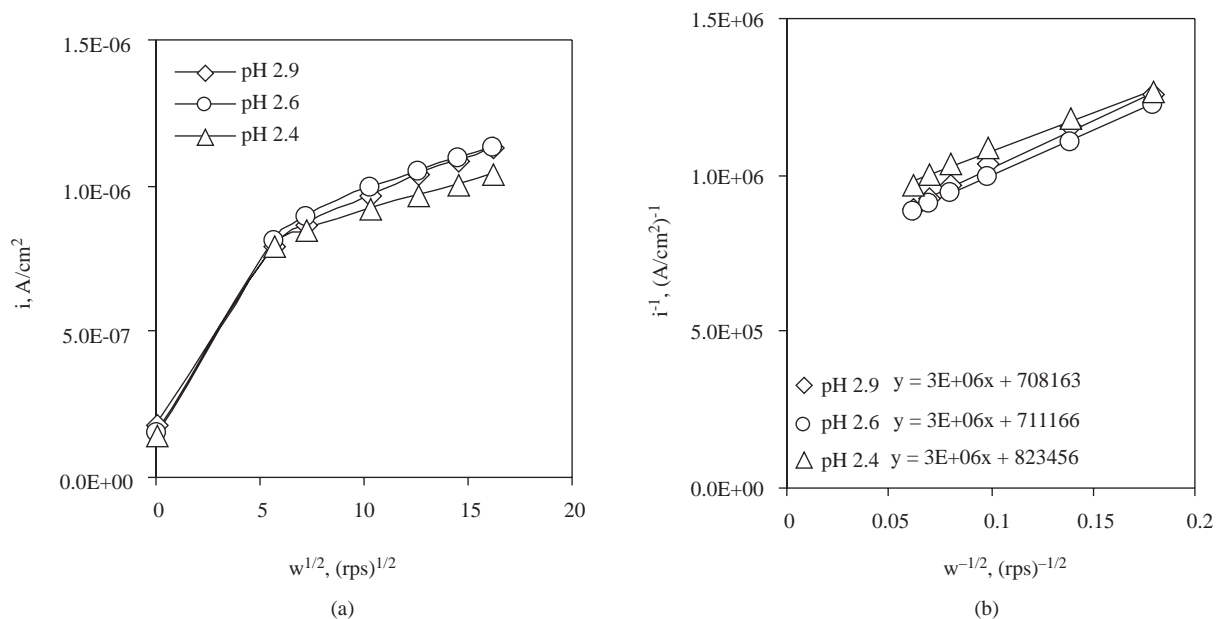


**Figure 9.** (a) Effect of specimen rotation on the steady-state currents in Region B. (b) Corresponding Koutecky-Levich plots.

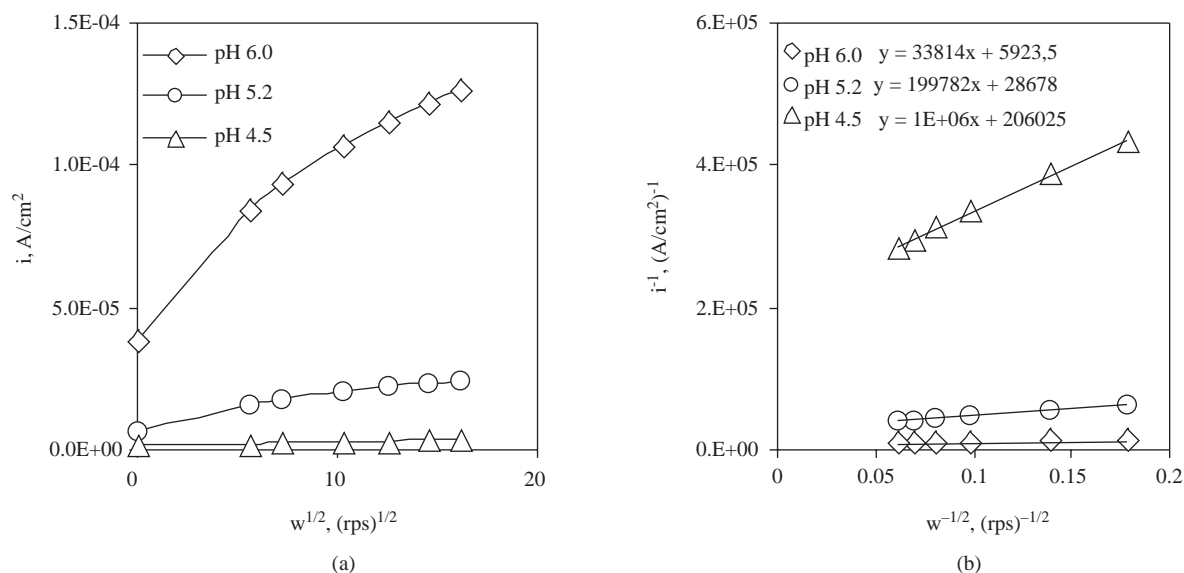


**Figure 10.** (a) Effect of specimen rotation on the steady-state currents in Region C. (b) Corresponding Koutecky-Levich plots.

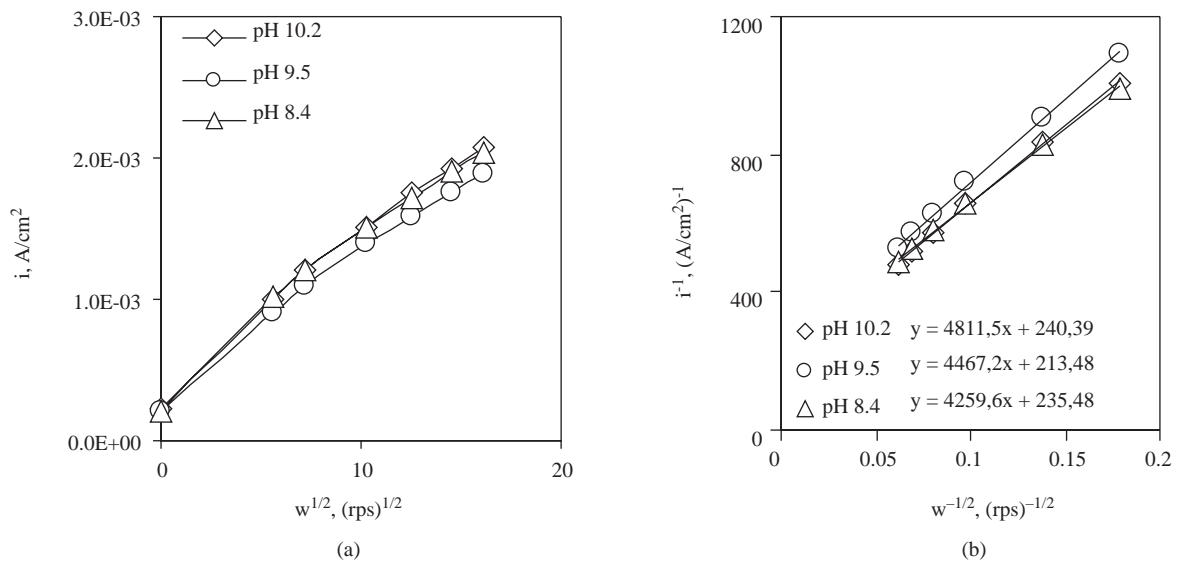


**Figure 11.** (a) Effect of specimen rotation on the steady-state currents in Region D. (b) Corresponding Koutecky-Levich plots.

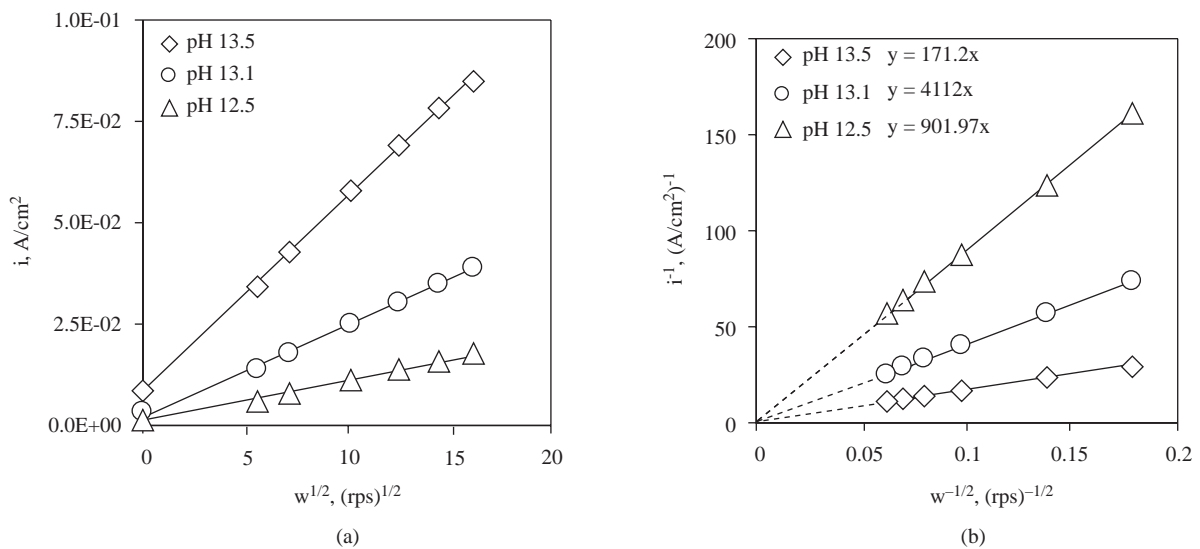


**Figure 12.** (a) Effect of specimen rotation on the steady-state currents in Region E. (b) Corresponding Koutecky-Levich plots.

The anodic currents exhibit an initial rise with rotation of the electrode from 0 to 300 rpm (300 rpm;  $w^{1/2} = 5.6 \text{ rps}^{1/2}$ ) in Figure 8a. A further increase in rotation, however, has almost no influence on the current. As pH decreases, the slopes of the lines in Figure 8b approach zero. This trend suggests that anodic current is mainly controlled by the kinetics of reaction<sup>12,13</sup> in Equation 2 in Region A. Therefore Equation 8 is not valid and Equation 9, where  $C$  is the surface  $\text{H}^+$  concentration, defines total anodic current in this pH regime. The initial rise with the application of rotation may result from the stabilization of the hydrodynamic conditions (e.g., the local pH on the electrode surface gets closer to the bulk pH<sup>14</sup>).

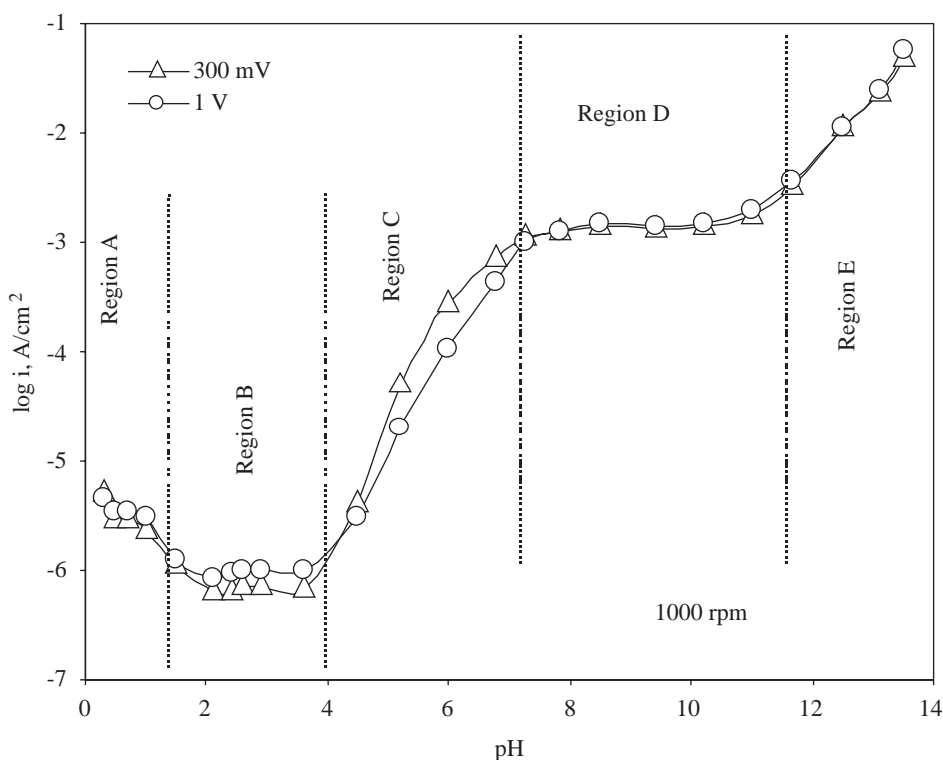


**Figure 13.** Effect of potential (pseudo plateau current region potentials: 300 mV and 1 V; Figure 3) on the steady-state currents obtained at 1000 rpm specimen rotation.

The initial rise with the rotation of an electrode from 0 to 300 rpm is more pronounced in Figure 9a. The increase in anodic current persists with a lower rate as the rotation increases. The sloped lines in Figure 9b suggest that current in Region B is under the mixed control of kinetics and diffusion as expressed by Equation 8<sup>12,13</sup>. The kinetic-controlled current is as in Equation 9, where  $C$  is the surface  $\text{H}_2\text{O}$  concentration in this pH regime according to the reaction in Equation 3. Diffusion control may result from either diffusion of oxidized species from the electrode surface to the bulk of solution or diffusion of reacting ions from the bulk of solution to the electrode surface. A slight variation in current with the applied potential in the pseudo plateau region for pH 2.6 in Figure 3 eliminates the possibility of diffusion control due to slow diffusion of any reacting ion from the bulk of solution to the electrode surface. The steady-state currents obtained at 300 mV and 1 V under 1000 rpm specimen rotation are also shown in Figure 13 for comparison. As noted before, the 300 mV and 1 V values belong to the plateau region in the potentiodynamic polarization curves in Figure 3. Obviously, the steady-state currents gathered at 2 different plateau region potentials (300 mV and 1 V) are different (currents obtained at 300 mV are lower) for Region B in Figure 13. These observations show that the diffusion dependence of the W anodic currents in Region B results from the slow diffusion of the oxidized species from the electrode surface to the bulk of solution.

The sharp initial rise in current in Figure 9a upon switching the specimen from stationary to rotating can be observed better in Figures 6 and 7 in Region B. This rise cannot be explained only by the stabilization of local pH. The hydrated oxide film ( $\text{WO}_3 \cdot \text{H}_2\text{O}(\text{s})$ ; Equation 3) thinning through damage by hydrodynamic effects should be the main reason as Lillard et al.<sup>8</sup> suggested. As the rotation speed of the specimen increases, the physical damage to the oxide phase may still have an effect. Slow diffusion of  $\text{H}_2\text{WO}_4(\text{aq})$  (Equation 3)

from the electrode surface to the bulk of solution, however, may contribute also to the diffusion control on the anodic currents at high rotations in Figure 9a. If this contribution exists, then the diffusion coefficient and concentration terms in Equation 10 should be the diffusion coefficient and concentration of  $\text{H}_2\text{WO}_4(\text{aq})$  in Region B.

Referring to Figures 10a and 10b, anodic current is again under the mixed control of kinetics and diffusion<sup>12,13</sup>. Since the anodic process in Region C is controlled by the reaction in Equation 4, the C term in the kinetic current expression in Equation 9 stands for the surface  $\text{OH}^-$  concentration in this pH regime. (Please note that the  $\text{OH}^-$  ions in Equation 4 refer to the adsorbed surface  $\text{OH}^-$  ions on the metal oxide surface. Therefore, above pzc normally the adsorbed surface  $\text{OH}^-$  ions play the prominent role in the dissolution, although the solution is acidic in Region C.) The potential dependence of the anodic currents in the plateau region in the potentiodynamic polarization curve for pH 5.2 in Figure 3 and that of steady-state currents in Region C in Figure 13 suggest that diffusion control stems from slow diffusion of surface  $\text{WO}_4^{2-}$  ions (Equation 4) to the bulk of solution. Therefore, the diffusion coefficient and concentration of  $\text{WO}_4^{2-}$  ions should be substituted into the diffusion current expression in Equation 10 for this pH regime.

Figures 11a and 11b show the mixed-controlled anodic process<sup>12,13</sup>. Diffusion control, however, seems more significant in this high current region (Region D) compared to previous regions (Regions B and C). There is no considerable influence of the applied potential on the plateau region currents of the potentiodynamic curve for pH 8.4 in Figure 3, and the steady-state currents are almost potential independent in Region D in Figure 13. The fact that current is pH independent in this pH regime (Figures 6 and 7), however, eliminates any possibility of diffusion-control originating from the slow diffusion of bulk  $\text{OH}^-$  ions. Therefore, diffusion control results from the slow diffusion of oxidized W species ( $\text{WO}_4^{2-}$ ; Equation 5) as Armstrong et al.<sup>5</sup> suggested. If currents are extrapolated to infinite rotation speed<sup>12,13</sup> ( $w \rightarrow \infty$ ) in Figure 11b, an almost constant kinetic current can be obtained for all pH values. Therefore, it may be convenient to eliminate the concentration term in the kinetic current expression in Equation 9 for this pH regime. Equation 10, however, can be modified with the substitution of the  $\text{WO}_4^{2-}$  ion diffusion coefficient and concentration.

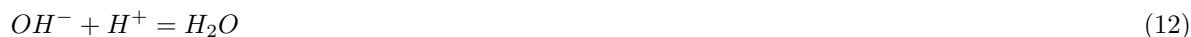
The anodic currents increase linearly with the increase in specimen rotation in Figure 12a and extrapolation of the currents to infinite rotation speed ( $w \rightarrow \infty$ ; dashed lines) shows all the lines to intersect at the origin in Figure 12b. This observation suggests that anodic current is under the total control of diffusion<sup>12,13</sup> in Region E. There is a very well-defined anodic limiting current for pH 13.5 in Figure 3 and the steady-state currents are potential independent in Region E in Figure 13. As pH increases, the steady-state currents also increase in Region E as depicted in Figures 6 and 7. All these results show that W anodic current in this pH regime is under the total control of the slow diffusion of  $\text{OH}^-$  ions (Equation 7) from the bulk of solution to the electrode surface, contrasting with the conclusion of Armstrong et al.<sup>5</sup> but confirming the proposals of Davydov et al.<sup>6,7</sup>.

According to Equations 8, 9 and 10, the slopes of the lines in Figures 9b, 10b, 11b and 12b can be expressed as in Equation 11:

$$\text{Slope} = (0.62nFD^{2/3}v^{-1/6}C)^{-1} \quad (11)$$

If the diffusing species is the  $\text{OH}^-$  ion in Region E, then the D and C terms in Equation 11 (also in Equation 10) should be the diffusion coefficient and bulk concentration of this ion, respectively. The bulk

concentration of the  $\text{OH}^-$  ion is mainly determined by the following reaction in the aqueous solution:



According to Reaction 12, bulk  $\text{OH}^-$  concentration can be defined as in Equation 13:

$$C_{\text{OH}} = \frac{a_{\text{H}_2\text{O}}}{\gamma_{\text{OH}} K a_{\text{H}}} \quad (13)$$

where  $a_{\text{H}_2\text{O}}$  and  $a_{\text{H}}$  are activities of  $\text{H}_2\text{O}$  and  $\text{H}^+$  ions, respectively,  $\gamma_{\text{OH}}$  is the activity coefficient of  $\text{OH}^-$  ions and  $K$  is the equilibrium constant of Reaction 12. Measured pH of the solution is related  $a_{\text{H}}$  as in Equation 14:

$$\text{pH} = -\log a_{\text{H}} \quad (14)$$

Combination of Equations 11, 13 and 14 results in Equation 15:

$$QD^{2/3} = (10^{\text{pH}} \text{ slope})^{-1} \quad (15)$$

where  $Q$  is defined as in Equation 16:

$$Q = 0.62nFv^{\frac{-1}{6}} \frac{a_{\text{H}_2\text{O}}}{K\gamma_{\text{OH}}} \quad (16)$$

The term  $Q$  is constant at fixed solution temperature ( $T = 20\text{ }^\circ\text{C}$ ) and ionic strength ( $I = 1.4$ ). If the diffusing species is the  $\text{OH}^-$  ion, then the diffusion coefficient ( $D$  term on the left-hand side of Equation 15) and thus the term on the right-hand side of Equation 15 must be constant for all pH values in Region E. This proposal is tested by the generation of pH vs.  $-\text{pH}-\log(\text{slope})$  curve as shown in Figure 14. The slope values in Figure 14 are picked from Figures 11b and 12b, and the comparison is made between Region D and Region E. It is apparent from Figure 14 that the term on the right-hand side of Equation 15 does not change with solution pH in Region E, in contrast to the trend in Region D. Obviously, the diffusing species in Region D ( $\text{WO}_4^{2-}$  ion) is different from the one in Region E ( $\text{OH}^-$  ion).

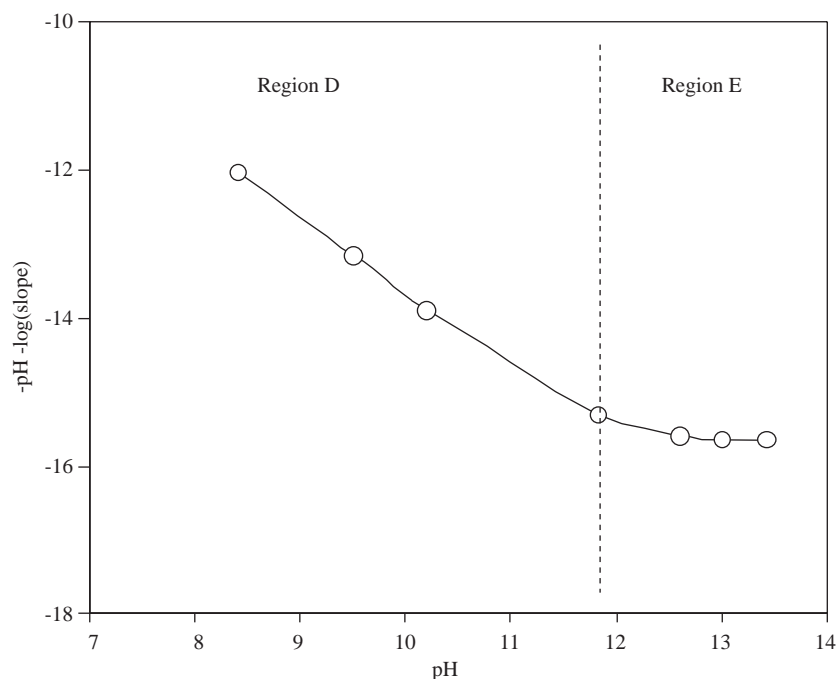


**Figure 14.** Variation of the term on the right-hand side of Equation 15 with pH in Regions D and E.

## Summary and Conclusions

The effect of diffusion on the anodic reactions of W was investigated in each pH regime and the following conclusions were drawn:

- In Region A, the anodic current was controlled mainly by the kinetics of  $H^+$ -assisted oxide dissolution.
- The kinetics of  $H_2O$ -assisted oxide dissolution were controlling the anodic current in Region B. The specimen rotation, however, was also found to affect the anodic reaction. This observation was mainly attributed to the physical damage to the hydrated oxide phase by hydrodynamic effects. The anodic process in this pH regime might also be influenced by slow diffusion of  $H_2WO_4(aq)$  from the electrode surface to the bulk of solution.
- The anodic current was under the mixed control of the kinetics of  $OH^-$ -assisted oxide dissolution and slow  $WO_4^{2-}$  ion diffusion from the metal surface to the bulk of solution in Region C.
- Mixed control of the kinetics of hydrated oxide ( $H_2WO_4(s)$ ) phase solubilization and slow  $WO_4^{2-}$  ion diffusion from the electrode surface were observed to affect the anodic process in Region D.
- Slow diffusion of  $OH^-$  ions from the bulk of solution to the electrode surface was totally controlling the anodic current of W in Region E.

## Acknowledgment

This work was supported by Osmangazi University Research Fund (No: 2001/14).

### References

1. M. Anik and K. Osseo-Asare, **J. Electrochem. Soc.**, **149**, B224-33 (2002).
2. M. Anik, **Turk. J. Chem.**, **26**, 915-24 (2002).
3. T. Heumann and N. Stolica, **Electrochim. Acta**, **16**, 643-51 (1971).
4. T. Heumann and N. Stolica, **Electrochim. Acta**, **16**, 1635-46 (1971).
5. R.D. Armstrong, K. Edmonson and R.E. Firman, **J. Electroanal. Chem.**, **40**, 19-29 (1972).
6. A.D. Davydov, V.S. Krylov and G.R. Engelhardt, **Elektrokhimiya**, **16**, 192-96 (1980).
7. A.D. Davydov, V.S. Shaldaev, A.N. Malofeeva and I.V. Savotio, **J. Appl. Electrochem.**, **27**, 351-54 (1997).
8. R.S. Lillard, G.S. Kanner and D.P. Butt, **J. Electrochem. Soc.**, **145**, 2718-25 (1998).
9. A.T. Vasko, in Encyclopedia of Electrochemistry of the Elements, ed., A.J. Bard, **Vol. 5**, pp. 69-130, Marcel Dekker, New York (1976).
10. G.S. Kelsey, **J. Electrochem. Soc.**, **124**, 814-19 (1977).
11. K.S. Pitzer, Activity Coefficients in Electrolyte Solutions, 2<sup>nd</sup> Ed., pp. 75-154, CRC Press, Boca Raton (1991).
12. Yu.V. Pleskov and V.Yu. Filinovskii, The Rotating Disc Electrode, pp. 25-75, Plenum, New York (1976).
13. A.J. Bard and L.R. Faulkner, Electrochemical Methods Fundamentals and Applications, 2<sup>nd</sup> Ed., pp. 331-50, John Wiley, New York (2001).
14. M. Anik and K. Osseo-Asare, in Chemical Mechanical Planarization IV, R.L. Opila, C. Reidsema-Simpson, K.B. Sundaram, and S. Seal, Editors, **PV 2000-26**, pp. 165-72, Electrochem. Soc. Proc. Series, Pennington, NJ (2001).